Signatures of an annular Fermi sea

Insun Jo, Yang Liu, L. N. Pfeiffer, K. W. West, K. W. Baldwin, M. Shayegan, and R. Winkler

Phys. Rev. B **95**, 035103 — Published 3 January 2017

DOI: 10.1103/PhysRevB.95.035103

Signatures of an annular Fermi sea

Insun Jo, Yang Liu, L. N. Pfeiffer, K. W. West, K. W. Baldwin, and M. Shayegan
Department of Electrical Engineering, Princeton University, Princeton, NJ 08544, USA

R. Winkler
Department of Physics, Northern Illinois University, Dekalb, IL 60115, USA

The concept of a Fermi surface, the constant-energy surface containing all the occupied electron states in momentum, or wavevector (k), space plays a key role in determining electronic properties of conductors. In two-dimensional (2D) carrier systems, the Fermi surface becomes a *contour* which, in the simplest case, encircles the occupied states. In this case, the area enclosed by the contour, which we refer to as Fermi sea (FS), is a simple disk. Here we report the observation of a FS with a new topology, namely a FS in the shape of an *annulus*. Such a FS is expected in a variety of 2D systems where the energy band dispersion supports a *ring of extrema* at finite k, but its experimental observation has been elusive. Our study provides: (1) theoretical evidence for the presence of an annular FS in 2D hole systems confined to wide GaAs quantum wells, and (2) experimental signatures of the onset of its occupation as an abrupt rise in the sample resistance, accompanied by a sudden appearance of Shubnikov-de Haas oscillations at an unexpectedly large frequency whose value does *not* simply correspond to the (negligible) density of holes contained within the annular FS.

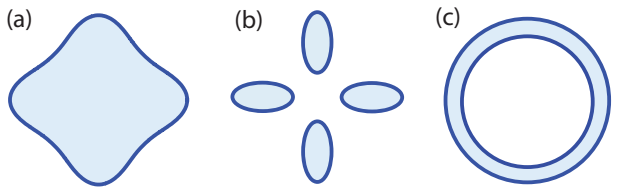

FIG. 1. Examples of Fermi seas in 2D systems: (a) simple disk, (b) multi-fold ellipses, (c) annulus.

Many properties of conductors are influenced by the shape, connectivity, and topology of their FS[1,2]. Figure 1 highlights examples of FSs in 2D systems. The simplest FS, a connected disk, is shown in Fig. 1(a). In 2D systems with multiple conduction band valleys, e.g. 2D electrons confined to Si or AlAs quantum wells (QWs)[3–5] or 2D electrons in a wide GaAs QW subject to very large parallel fields[6], the FS consists of a number of separate sections, each containing a fraction of the electrons in the system (Fig. 1(b)). Figure 1(c) shows yet another possible FS topology, namely an *annulus*, which is the subject of our study. The existence of such a FS, emerging from an inverted energy band with a ring of extrema at finite k, has been discussed for many systems; e.g., those with a strong spin-orbit interaction (SOI)[7–14], biased bilayer graphene[15–19], or monolayer gallium chalcogenides[20,21]. Moreover, since the electron states near the band extremum become highly degenerate, resulting in a van Hove singularity in the density of states, an annular FS has been predicted to host exotic interaction-induced phenomena and phases such as ferromagnetism[19–21], anisotropic Wigner crystal and nematic phases[22–26], and a persistent current state[18].

Although the possibility of an annular FS has long been recognized theoretically, its experimental detection has been elusive. For cases (a) and (b) in Fig. 1, the FS can readily be probed via magneto-transport measurements as the frequencies of the Shubnikov-de Haas (SdH) oscillations, multiplied by e/h, directly give the FS area or, equivalently, the areal density of the 2D system[4–6,27–29]; e is electron charge and h is the Planck constant. For the annular FS of case (c), however, no data have been reported. Nor is it known how the SdH oscillations should behave, or how their frequencies are related to the area of the annular FS. Here we report energy band calculations and experimental data, demonstrating the realization of an annular FS and its unusual SdH oscillations in 2D hole systems (2DHSs) confined in wide GaAs QWs.

Figure 2 captures the key points of our study. Figures 2(a) and 2(b) show the calculated energy band dispersions for a 2DHS at a density of $p = 1.20\times10^{11}$ cm^{-2} confined in a 38-nm-wide GaAs QW. The self-consistent calculations are based on the 8×8 Kane Hamiltonian[14]. The charge distribution is bilayer-like (Fig. 2(d)) because the Coulomb repulsion pushes the carriers (holes) towards the confinement walls[30–32]. As seen in Figs. 2(a) and (b), the energy band dispersion is very unusual, showing an *inverted* structure for the excited subband with a "ring of maxima" at finite values of k. So far, such dispersions were studied mostly within systems with the Rashba SOI[7–12,14]. However, in our symmetric 2DHS (without the Rashba SOI), the inverted band structure stems from the combined effect of a strong level repulsion between the second heavy-hole and the first light-hole subbands at $k > 0$[33] as well as the Dresselhaus SOI[34]. Because such a band structure exists near the bottom of the excited subband, it is experimentally accessible at a moderate density of carriers in wide QWs. Additionally, high-density carriers in the ground subband screen the ionized impurity scattering so that carriers in the excited subband can have a relatively high mobility even

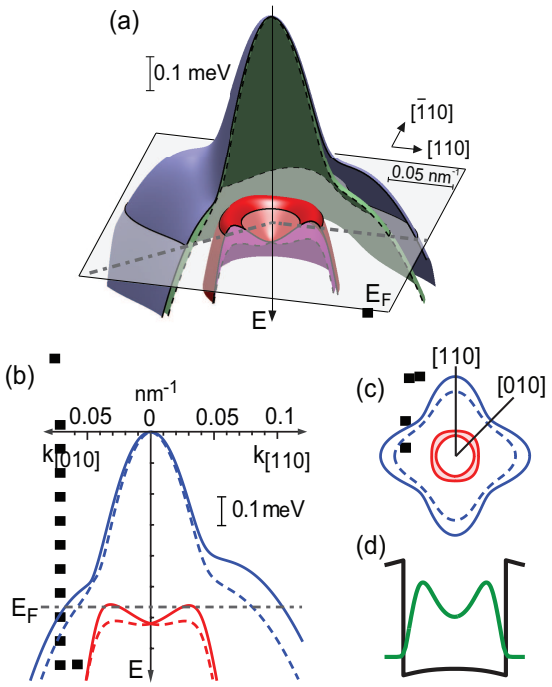

FIG. 2. (a) and (b) Calculated subband energy dispersions for GaAs 2D holes in a 38-nm-wide GaAs QW at density $p = 1.2 \times 10^{11}$ cm^{-2}. The upper (lower) dispersions are for the ground (excited) subbands, each consisting of two spin-split branches at finite k, shown by solid and dashed lines. The horizontally-cut plane in (a) and the dash-dotted line in (b) mark the Fermi energy. In (b) the energy dispersions are shown along two directions. (c) Fermi contours for the ground (blue) and excited (red) subband. The FSs for the ground subband are not filled with color for clarity; the FS for the excited subband is the red annulus. (d) Hole charge distribution (green) and potential (black).

at a low density. When holes start to occupy the excited subband, its FS adopts an annular shape (Fig. 2(c)). Unlike the FS of the ground subband, the annular FS has a void for small k. In our experiments we probe the energy band dispersions via monitoring the sample resistance and also measuring SdH oscillations as a function of density. As the holes start to occupy the excited subband, we observe an abrupt rise in the sample resistance, and a sudden appearance of an extra peak at a relatively large frequency in the Fourier transform (FT) spectra. We associate this peak with the annular FS, and discuss the details of its evolution with increasing hole density.

We used 40- and 35-nm-wide, symmetric, GaAs QWs grown by molecular beam epitaxy along the [001] crystal direction. Here we focus on data for the 40-nm-wide QW; we observe qualitatively similar data for the narrower QW, as presented in Appendix IV. The QWs are symmetrically modulation doped with two C δ-layers. We used two 40-nm-wide QW samples with different $Al_{0.3}Ga_{0.7}As$ spacer-layer thicknesses (160 and 90 nm), different as-grown hole densities ($p = 1.3$ and 2.0, in units of 10^{11} cm^{-2} which we use throughout this manuscript), and mobilities (32 and 76 m^2/Vs). The data for $p \leq 1.43$ are taken from the lower density sample, and the higher density data from the other sample. In each sample, front- and back-gate electrodes allow us to change independently the 2D hole density and the asymmetry of the charge distribution in the QW. In this study, we focus on symmetric charge distributions; we judge the symmetry via a careful examination of the SdH oscillations in the low-density regime where only the ground subband is occupied[35], as well as the strengths of fractional quantum Hall states, e.g. at $\nu = 1/2$[32]. The low-field magneto-resistance oscillations are measured in a dilution refrigerator at a base temperature of $\sim$50 mK.

Figure 3 shows the evolutions of: (a) low-field magneto-resistance data, (b) their corresponding FT spectra, (c) the calculated energy dispersions, and (d) the associated Fermi contours[36]. For clarity, the traces in Fig. 3(a) and their FTs in Fig. 3(b) are shifted vertically. The intensities of the FTs are normalized so that the heights of the strongest FT peaks in different spectra are comparable. For all traces the total density is determined from the position of the high-frequency peak that is marked by an empty circle following Onsager[28], i.e., by multiplying the frequency by e/h. This density agrees, to within 4%, with the magnetic field positions of the integer and fractional quantum Hall states observed at high fields. At low densities ($p < 1.2$) the FT spectra are simple. Besides a peak corresponding to the total density, we also observe a second peak, marked by a blue closed circle, at half value of the total density peak. We associate this peak with SdH oscillations at very low magnetic fields where the Zeeman energy is small and the spin splitting of the ground subband Landau levels is not yet resolved.

As the density is raised to $p = 1.20$, a FT peak suddenly appears at $\simeq$1.5 T in Fig. 3(b). This peak, which is marked by a red arrow and circle in the $p = 1.20$ trace, signals the onset of the excited-subband occupation[37]. As we discuss later, there is also a rather sharp rise in the sample resistance at $p = 1.20$ (Fig. 4), consistent with our conjecture. This new FT peak has two unusual characteristics. First, its emergence is very abrupt. It is essentially absent at a slightly lower density of $p = 1.16$, and its strength grows very quickly to become the dominant peak in the whole FT spectrum at a slightly higher density of $p = 1.25$. Second, its frequency, multiplied by the usual factors (e/h or $2e/h$), clearly does *not* give the correct density of holes in the excited subband, which we expect to be extremely small, essentially zero at the onset of excited subband occupation. Consistent with this expectation, the peak near 2.5 T (marked by a blue circle), which we associate with the ground subband, indeed accounts for essentially *all* the QW's holes: 2.5 T multiplied by $2e/h$ gives $p = 1.20$, leaving very few holes for the excited subband. Hence we conclude that the frequency of the $f \simeq 1.5$ T peak is not simply related to

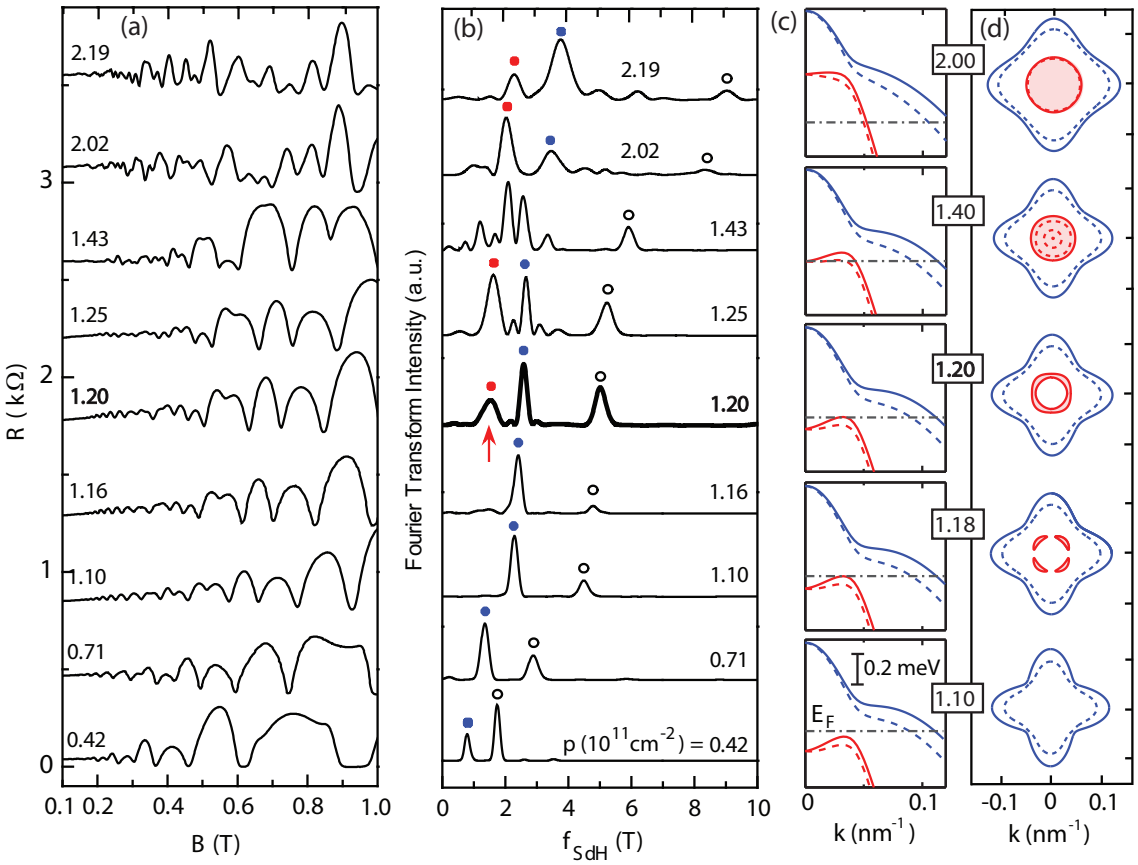

FIG. 3. (a) Low-field magneto-resistance traces at different densities. (b) Fourier transform spectra of the SdH oscillations at each density. Open circles indicate total density peaks. Blue and red circles mark the peaks associated with the ground and excited subbands; respectively. (c) Calculated energy dispersions and, (d) Fermi sea, at densities $p = 1.10, 1.18, 1.20, 1.40, 2.00 \times 10^{11}$ cm^{-2}, from bottom to top. Gray dash-dotted lines in (c) represent the Fermi energy. In (c) and (d), blue and red lines correspond to the ground and excited subbands, respectively; solid and dashed lines represent the spin-split states.

the excited-subband density. This is in sharp contrast to the GaAs 2D *electron* systems where, after the onset of the excited-subband occupation, a FT peak appears at a small frequency which correctly gives the electron density of the excited subband, and this peak's frequency increases slowly and continuously as more electrons occupy the excited subband[27,38–42].

We associate the $f \simeq 1.5$ T peak appearing at the onset of the excited-subband occupation with the formation of an annular FS in our 2DHS. But, how should an annular FS be manifested in SdH oscillations? Given that the frequency of this peak does not correspond to the area of the annulus, is there an alternative relation? Following Onsager[28], one may conjecture that it could lead to oscillations whose frequencies are given by the areas enclosed by the outer and inner circles (or more generally, the "contours") of the annulus, namely by the areas πk_o^2 and πk_i^2, where k_o and k_i are the radii of the outer and inner circles (see the Fermi contour for $p = 1.20$ in Fig. 3(d).) Near the onset of the excited-subband occupation, the outer and inner contours of the annulus are very close to each other, implying that the FT should show two closely-spaced peaks, or one broad peak (if these two peaks cannot be resolved), qualitatively consistent with our data. Quantitatively, based on the energy band calculations for $p = 1.20$, we would expect FT peaks at $f = 0.43$ T and $f = 0.27$ T for the outer and inner rings, respectively. These values are smaller than the frequency ($f \simeq 1.5$ T) of the broad peak we observe in the FT. This discrepancy might imply that the semi-classical description is not entirely correct, or that the band calculations without considering the exchange energy are not quantitatively accurate near the bottom of the excited subband. Additionally, quantum mechanical effects for a k-space trajectory in the annulus can cause corrections to the semi-classical description of the SdH oscillations[43–45].

The evolution of the FT spectra for $p > 1.20$ is also suggestive. For $p = 1.43$, e.g., the spectrum becomes quite complex, showing multiple peaks near 2 T. This

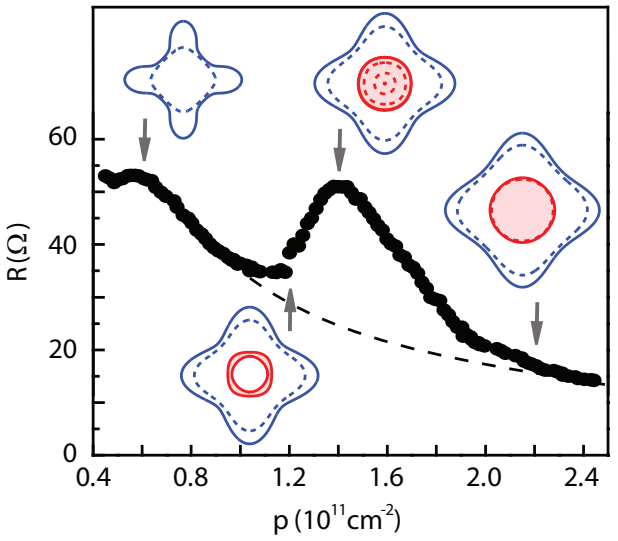

FIG. 4. Zero-field resistance as a function of density. Fermi seas are shown for four densities indicated by arrows. The dashed line is a guide to the eye.

is qualitatively consistent with the results of the energy band calculations: Near the onset of the excited-subband occupation, E_F can have four crossings with the excited-subband dispersion (two for each spin-subband dispersion), resulting in two, complex annular FSs (see Figs. 3(c) and (d) for $p = 1.40$). As we further increase the density, the FT spectra become simpler, showing two dominant peaks at the highest densities (see FTs for $p = 2.02$ and 2.19 in Fig. 3(b)). Such an evolution qualitatively agrees with our expectation based on the calculated bands, which indicate two "disk-like" FSs (i.e., without voids at $k = 0$), one for each subband. Also consistent with calculations, these peaks move to higher frequencies when the densities of subbands increase with increasing total density. If we assign these peaks to the areas of the FSs for the ground and excited subbands, multiply their frequencies by $2e/h$, and sum the two densities, we find a total density which is $\sim 30\%$ larger than the total density expected from the open circles. If we assume that the excited-subband Landau levels are spin-resolved, and multiply the lower frequency (red) peak by e/h (instead of $2e/h$), then we obtain a total density which agrees to better than $\sim 8\%$ with the total density deduced from the open circles.

We also measured the zero-field resistance of the 2DHS as a function of the total density in the QW. The data, shown in Fig. 4, provide corroborating, albeit indirect, evidence for our conclusions. At low densities ($p < 1.2$) where only the ground subband is occupied, the resistance decreases with increasing density, consistent with an increase in conductivity because of the larger hole density and higher mobility. At $p \simeq 1.2$, the resistance shows an abrupt and significant increase. A qualitatively similar rise is also seen at the onset of the occupation of the excited subband in GaAs 2D electrons[38–40], and can be attributed to the enhanced inter-subband scattering. In Fig. 4, the resistance remains high in the density range $1.2 < p < 1.8$ where in our experiments we oberve multiple, anomalous peaks in the FT spectra (see, e.g., data for $p = 1.25$ and 1.43 in Fig. 3(b)). For $p \geq 1.8$, the resistance returns to low values as the SdH oscillaions and their FTs become simple again, signaling that E_F has gone past the inverted band dispersion.

Before closing, we make two remarks. First, right at the onset of the excited-subband occupation and in an extremely narrow density range near $p = 1.18$, the calculated FS of the excited-subband consists of four "arcs" (see Fig. 3(d)). We do not seem to observe a signature of such a FS in SdH measurements, likely because of the extremely small density of holes in the arcs, and also because of the very narrow density range where the arcs prevail. Second, techniques such as angle-resolved photo-emission spectroscopy (ARPES) could in principle be used to probe the annular FS we study. However, the relevant energy scale of the inverted energy band we are probing is only ~ 0.1 meV (see Fig. 2(b)), well below the energy resolution of state-of-the-art ARPES measurements (~ 1 meV)[46]. Our SdH data therefore provide a unique probe of such annular FSs.

In conclusion, our study of low-field SdH oscillations for 2D holes confined in a wide QW reveals signatures of an annular FS that originates from the inverted dispersion of the excited subband. When the excited subband begins to be populated, in the FT spectrum we observe a sudden emergence of an anomalous peak whose frequency is not associated with the density of holes in the excited subband through the usual Onsager relation. We add that near the onset of this population, the holes in the excited subband occupy only one spin branch of the dispersion. This is qualitatively different from the usual case (e.g., the ground subband) where, in the absence of the linear-k SOI, the holes occupy both spin-subbands even at the onset of the occupation. Our results should stimulate future experimental and theoretical studies of the unusual dispersion and annular FS.

Appendix I: Contrast between Fermi seas for 2D electrons and holes

Two-subband systems containing high mobility two-dimensional (2D) electrons confined in a GaAs quantum well (QW) have been studied previously[29,38–42,47]. Since the energy dispersions of both ground and excited subbands are parabolic, the Fermi seas are simple, circular disks in a wide density range. In Fig. A1, we schematically show the energy dispersions for (a) electrons and (b) holes, and the shapes of their Fermi seas. In wide QWs, where the energy separation between the ground and excited subbands is small, the Fermi energy (E_F), denoted by grey dash-dotted lines in Fig. A1, can be tuned to reach the excited subband by increasing the density of carriers. In Fig. A1, E_F for three representative regimes is shown: (i) E_F is located in the ground subband, (ii) E_F is just past the edge of the excited subband, (iii) E_F is well beyond the onset of the excited subband occupation. For each regime, the shapes of Fermi seas for the ground (blue) and excited (red) subbands are shown in the right panels. The focus of our study is in regime (ii) where the annular Fermi sea develops for the case of holes (Fig. A1(b)). In contrast, for electrons, the shape of the Fermi sea is always circular for both the ground and excited subbands.

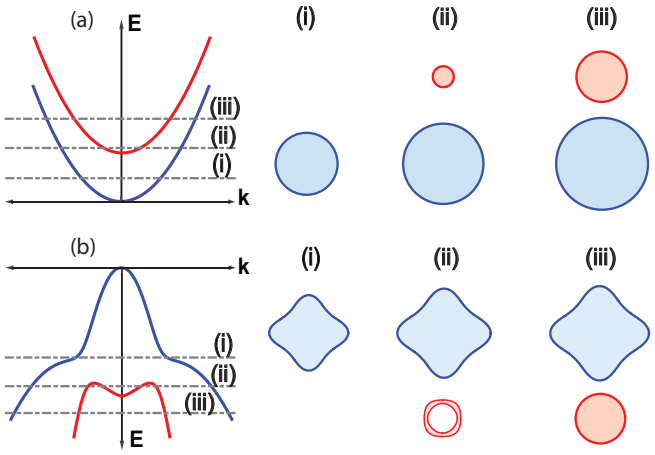

FIG. A1. Schematic energy dispersions for (a) electrons and (b) holes confined to wide GaAs QWs. Blue (red) curve represents the ground (excited) subband. Grey dash-dotted lines show different positions of the Fermi energy.

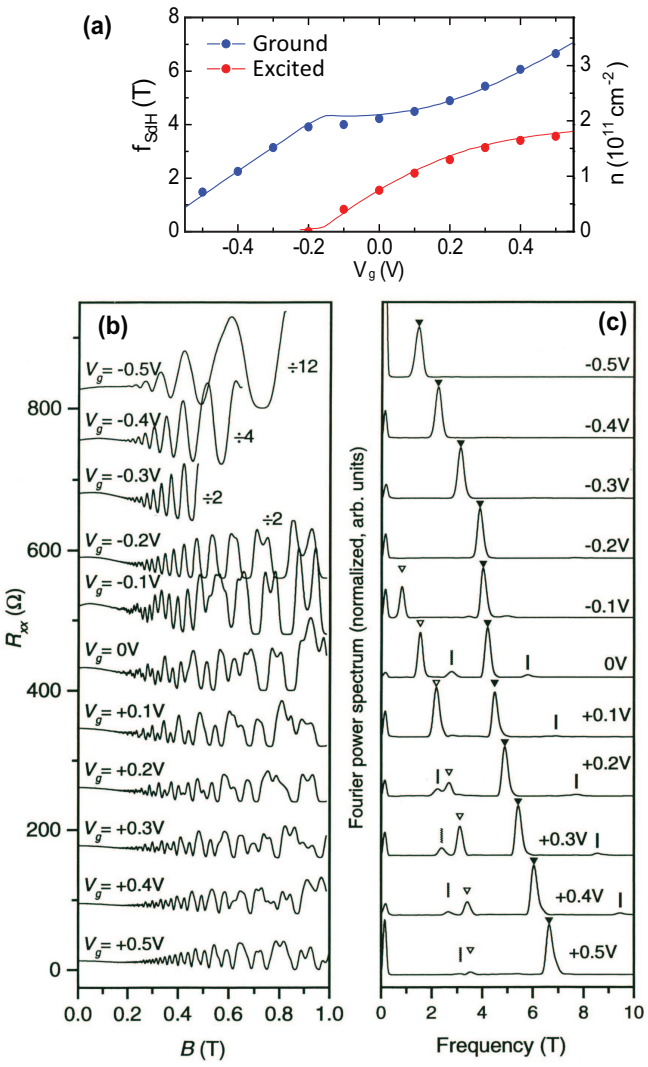

FIG. A2. (a) Summary of FT frequencies measured for 2D electrons confined in a 45-nm-wide GaAs QW at different front-gate voltages (V_g). The ground and excited subband densities are obtained by multiplying $2e/h$ and f_{SdH}. The red and blue lines represent the results of self-consistent, local-density-approximation calculations. (b) Low-field SdH oscillations measured at different V_g. Increasing V_g increases the density and therefore E_F. (c) FT spectra of the corresponding traces in (b) are shown. The closed (open) triangles mark the spin-unresolved peak of the ground (excited) subband. Vertical lines indicate the sum and/or difference of the two prominent peaks. The data are taken from Ref.[40].

Appendix II: Two-subband *electron* system with circular Fermi seas

The Shubnikov-de Haas (SdH) oscillations data and their Fourier transform (FT) spectra for 2D *electrons* confined in a 45-nm-wide GaAs QW are shown in Figs. A2(b) and (c), respectively[40], together with a summary plot in Fig. A2(a). A front-gate voltage, V_g, is applied to change the density, or E_F. The traces for $V_g \leq -0.2$ V show simple FT spectra, each with a single peak, marked by a closed triangle. This peak corresponds to the spin-unresolved carriers (i.e. $n = 2(e/h)f_{SdH}$). (Because of the small g-factor for GaAs 2D electrons, Zeeman spin-splitting is not present in the low field range used for the FT analysis, leading to the absence of a spin-resolved peak in the FT spectra.) When $V_g \geq -0.1$ V, E_F moves

past the bottom of the excited subband (case (ii) in Fig. A1(a)). As a result, a FT peak corresponding to the excited subband appears at $\simeq 0.8$ T, as marked by an open triangle at $V_g = -0.1$ V in Fig. A2(c). As the density increases further, both peak positions move toward higher frequencies. The two FT peaks represent the densities of electrons in the ground and excited subband, and the sum of the two densities agrees very well with the total density in the entire density range[40,41]. The lines drawn through the data points in Fig. A2(a) are the results of self-consistent, local-density-approximation calculations. They agree quite well with the measured data.

Other small peaks, marked by vertical lines, are also observed at the sum and difference of the two major peak positions. The frequency corresponding to the sum of two major peak frequencies is expected when the Landau levels are sharp[48]. The frequency corresponding to the difference of two major peak frequencies can be explained by the inter-subband scattering[49].

As we emphasize in the main text, there are distinct characteristics observed in the FT spectra of circular vs. annular Fermi sea for the excited subband of 2D electrons and holes. 2D electrons, forming only *circular* Fermi seas as shown in Fig. A1(a), exhibit a smooth transition of the FT frequencies (see Figs. A2(a) and (c)). Also, the total density always agrees with the sum of the two frequencies multiplied by $2e/h$, following the Onsarger's relation[28]. In contrast, in the case of the annular Fermi sea, an anomalous FT peak appears abruptly at a finite frequency. Moreover, the sum of the FT frequencies is larger than the total density peak position when the annular Fermi sea develops (see Figs. 3(b) and (c)).

Appendix III: Shubnikov-de Haas oscillations of an annular Fermi sea via inverse Fourier transform

In Fig. 3(b), we observe a finite-frequency peak at $f \simeq 1.5$ T in the FT of SdH oscillations for our 2D hole system at $p = 1.20$ (p is the total 2D hole density in units of 10^{11} cm^{-2}). We associate this peak with the onset of excited subband occupation and the resulting annular Fermi sea. Here we demonstrate that the SdH oscillations corresponding to the annular Femi sea exhibit clear low-field oscillations, which are nearly periodic in $1/B$. In order to extract the SdH oscillations induced by the annular Fermi sea, we perform *inverse* FTs for individual peaks as shown in Fig. A3.

In Fig. A3, we show two examples of inverse FT analyses performed at $p = 1.10$ and 1.20. Figures A3(a-c) are for $p = 1.10$ and Figs. A3(d-f) for $p = 1.20$.

When only the ground subband is occupied ($p = 1.10$), we observe two peaks in the FT spectrum (Fig. A3(a)); the lower (higher) frequency peak corresponds to the spin-unresolved (spin-resolved) SdH oscillations. The observation of the spin-resolved peak stems from the Zeeman spin-splitting in the field range where the SdH oscillations are analyzed. We apply a square window function to each peak and perform inverse FT separately. The results are shown in Fig. A3(b), where the green (blue) curve represents spin-resolved (spin-unresolved) SdH oscillations. The oscillations are periodic in $1/B$ for each curve, and the period of the green curve is twice the period of the blue curve. As shown in Fig. A3(c), when these two primary oscillations are added to produce the resulting SdH oscillations (orange curve), it agrees very well with the measured data (black curve).

For $p = 1.20$, near the onset of the excited subband occupation, we observe three major peaks in the FT spectrum (Fig. A3(d)). Two peaks (marked by the blue and green windows in Fig. A3(d)) are associated with the ground subband, while a peak marked by red window is from the excited subband. In Fig. A3(e), the inverse FTs of these peaks are shown in their respective colors. The blue and green curves in Fig. A3(e) are qualitatively similar to those in Fig. A3(b) except for the slightly smaller periods of the oscillations, consistent with the 10% larger density of the ground subband (1.20 compared to 1.10). In Fig. A3(e), we also show (red curve) the inverse FT of the anomalous peak (red window) in Fig. A3(d) which we associate with the excited subband. We find that the red curve in Fig. A3(e) is indeed reasonably periodic in $1/B$, except that its period varies between 1.4 and 1.8 T in the range $1 < 1/B < 5$ T^{-1}. This variation is consistent with the excited subband peak in Fig. A3(d) being broad compared to the other two (ground subband) peaks in the same FT spectrum. We note that the extra width of this peak is not due to its small frequency ($\sim$1.5 T); as seen in Fig. 3, the peak marked with the blue circle for $p = 0.71$ has a similar frequency but is much narrower.

It is not obvious what causes the extra broadening of the excited subband peak. As we state in the main text, it might be that there are two peaks (corresponding to areas enclosed by the outer and inner contours of the annular Fermi sea), and that we cannot resolve the two peaks. Another possibility is the "magnetic blurring" as discussed in Ref.[44]. When the area of annular Fermi sea is smaller than the square of the inverse magnetic length, the momentum space area can be blurred[44]. If we compare the momentum space area of the annular Fermi sea at $p = 1.20$ with $(1/l_B)^2$, such a blurring could happen for $B > 1.0$ T. Because the field range we use for FT analysis is less than 1.0 T, this blurring should not be relevant for our sample. On the other hand, if we use the criterion that the $k_o - k_i > 1/l_B$, then we conclude that based on the energy band calculations for $p = 1.20$ which predict $k_o - k_i = 0.0086$ nm^{-1}, there should be magnetic blurring for B > 0.04 T, i.e., that there should be corrections in the entire range of our measurements. Similarly, for $p = 1.25$ where $k_o - k_i = 0.017$ nm^{-1}, the magnetic blurring should affect the SdH oscillations for $B > 0.19$ T.

We conclude that the inverse FT technique we present here effectively extracts the SdH oscillations originating from the annular Fermi sea of the excited subband.

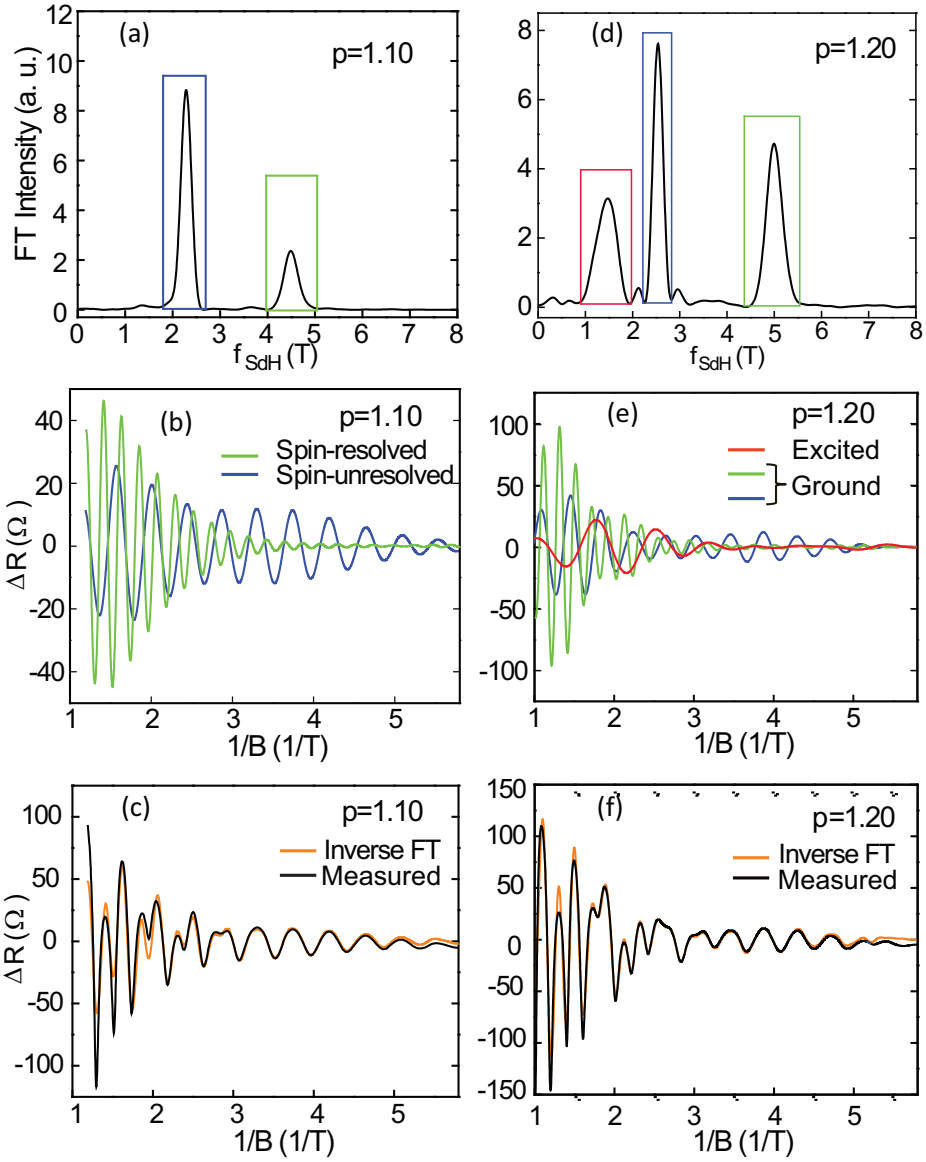

FIG. A3. (a) FT spectrum of SdH oscillations at $p = 1.10$ for the 40-nm-wide GaAs QW presented in the main text. Color-coded boxes indicate the square window function applied before implementing inverse FT. (b) Results of inverse FT for each peak are shown. Spin-resolved (spin-unresolved) SdH oscillations are constructed by using the total (half-density) peak in (a). (c) Sum of the two curves in (b) gives the full SdH oscillations (orange curve). Measured data (black) after a background subtraction are shown for comparison. (d) FT spectrum of SdH oscillations at $p = 1.20$. The additional peak associated with the annular Fermi sea is seen at $f \simeq 1.5$ T. (e) SdH oscillations for the ground and excited subbands are obtained after performing inverse FT of the peaks marked with boxes in (d): blue and green for the spin-unresolved and spin-resolved oscillations of the ground subband, and red for the excited subnand. (f) The sum of the three curves in (e) is shown as an orange curve and is compared with the measured data (black curve).

Appendix IV: Results for 2D holes confined to a 35-nm-wide GaAs QW

We also made measurements on a 35-nm-wide QW and observed similar signatures of an annular Fermi sea as summarized in Fig. A4. The QW structure is similar to that of the 40-nm-QW, and the density of the as-grown sample is $p = 1.63$. Using the front- and back-gates, we tune the density while keeping the charge distribution of the QW symmetric. We show FT spectra of the SdH oscillations at different densities in Fig. A4(a). Panels in Figs. A4(b) and (c) show the energy dispersions and the Fermi contours for three representative densities, $p = 1.40, 1.60, 2.00$. Numerical calculations for this narrower QW also indicate the presence of an annular Fermi sea near the onset of the excited subband occupation.

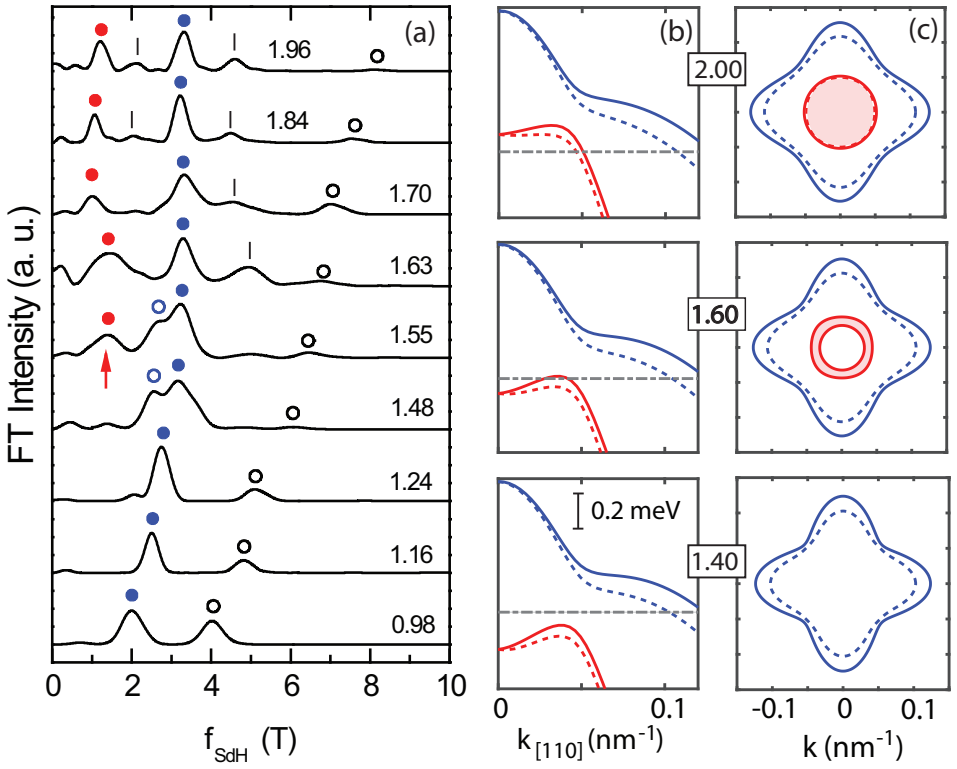

FIG. A4. (a) Fourier transform spectra of the SdH oscillations at different densities measured for 2D holes confined in a 35-nm-wide GaAs QW. Blue (red) circles mark the peaks associated with the ground (excited) subband, while open circles indicate the total density peaks. Vertical lines indicate the sum and/or difference of the two prominent peaks. (b) Calculated energy dispersions, and (c) Fermi contours at densities $p = 1.40, 1.60$, and 2.00. Blue (red) lines represent ground (excited) subband. Calculations were performed for a slightly narrower QW, of width 34 nm, to match the measured onset of the excited subband occupation.

The evolution of FT spectra of the SdH oscillations is shown in Fig. A4(a). At low densities, $p \leq 1.24$, the FT spectra show two peaks representing the spin-unresolved (blue circles) and spin-resolved (black empty circles) SdH oscillations for the ground subband, respectively. When $p = 1.48$, we observe a splitting of the ground subband peak, suggesting that the ground subband SdH oscillations become spin-resolved. When the density is increased to $p = 1.55$, an additional broad peak appears at $f \simeq 1.4$ T, indicated by a red arrow, which we associate with the annular Fermi sea in the excited subband. This peak persists and becomes stronger at $p = 1.63$. This anomalous peak exhibits two distinct features, similar to what we observe for the 40-nm-wide QW: (i) The peak appears abruptly at a finite frequency. (ii) The frequency of the peak does *not* correspond to the excited subband density (if we use the Onsager relation) when the annular Fermi sea is formed.

When the density increases further, the anomalous peak shifts to a slightly smaller value, marked by red circles. This peak grows slowly and continuously with increasing density, and eventually represents the density of the excited subband when its Fermi sea becomes a simple disk ($p \geq 1.84$).

We also find some differences between the two samples with different well widths. Compared to the 40-nm-wide QW, the onset of the excited subband occupation occurs at a higher density $p = 1.55$ for the 35-nm-wide QW. This is expected because the energy separation between the ground and excited subband is larger for a narrower QW. In addition, the finite frequency peak for the 35-nm-wide QW is seen at $f \simeq 1.4$ T, which is slightly smaller than $f \simeq 1.5$ T we observe for the 40-nm-wide QW. The energy band calculations shown in Fig. A4(b) are also consistent with our observations. Compared to the 40-nm-wide QW, the outer radius of the annulus at the onset of the excited subband occupation is about 8% smaller for the 35-nm-wide QW.

In the FT spectra for $p = 1.48$ and 1.55 in Fig. A4(a), we also observe a splitting of ground subband peak; we mark this splitting by the closed and open blue circles in these two spectra. Such a splitting is indeed expected from our energy band calculations (see the solid and dashed Fermi contours in Fig. A4(c)). However, it is unclear why we do not observe a similar splitting for the 40-nm-wide QW sample (Fig. 3(b)). Also, in Fig. A4(a), there are some extra peaks for $p \geq 1.63$, which we mark by vertical lines. These can be associated with

sums and/or differences of the main peaks (marked by red and blue circles), qualitatively similar to the 2D electron data (see Fig. A2(c)).

Despite the differences between the data for the 40- and 35-nm-wide QW samples, the clear common feature is the sudden appearance of a broad FT peak at a relatively large frequency ($\simeq 1.5$ T) when the upper subband starts to become occupied. This is the main feature we are associating with the annular Fermi sea.

ACKNOWLEDGMENTS

We acknowledge support by the DOE BES (DE-FG02-00-ER45841) grant for measurements, and the NSF (Grants DMR-1305691, DMR-1310199 and MRSEC DMR-1420541), the Gordon and Betty Moore Foundation (Grant GBMF4420), and Keck Foundation for sample fabrication and characterization. We also acknowledge support by the NSF for low-temperature equipment (Grant DMR-MRI-1126061). We appreciate stimulating discussions with S. Chesi, D. Culcer, R. J. Joynt, J. Jung, L. Smrcka, K. Vyborny, and U. Zülicke.

[1] N. W. Ashcroft and N. D. Mermin, *Solid State Physics* (Holt, Rinehart and Winston, Philadelphia, 1976).
[2] I. M. Lifshitz, J. Exptl. Theoret. Phys. **38**, 1569 (1960).
[3] K. Takashina, Y. Ono, A. Fujiwara, Y. Takahashi, and Y. Hirayama, Phys. Rev. Lett. **96**, 236801 (2006).
[4] Y. P. Shkolnikov, E. P. De Poortere, E. Tutuc, and M. Shayegan, Phys. Rev. Lett. **89**, 226805 (2002).
[5] O. Gunawan, Y. P. Shkolnikov, E. P. De Poortere, E. Tutuc, and M. Shayegan, Phys. Rev. Lett. **93**, 246603 (2004).
[6] M. A. Mueed, D. Kamburov, M. Shayegan, L. N. Pfeiffer, K. W. West, K. W. Baldwin, and R. Winkler, Phys. Rev. Lett. **114**, 236404 (2015).
[7] F. T. Vas'ko and N. A. Prima, Sov. Phys.–Solid State **21**, 994 (1979).
[8] Y. A. Bychkov and E. I. Rashba, JETP Lett. **39**, 78 (1984).
[9] E. Cappelluti, C. Grimaldi, and F. Marsiglio, Phys. Rev. Lett. **98**, 167002 (2007).
[10] L. W. Cheuk, A. T. Sommer, Z. Hadzibabic, T. Yefsah, W. S. Bakr, and M. W. Zwierlein, Phys. Rev. Lett. **109**, 095302 (2012).
[11] G. Bihlmayer, O. Rader, and R. Winkler, New J. Phys. **17** 050202 (2015).
[12] V. Brosco, L. Benfatto, E. Cappelluti, and C. Grimaldi, Phys. Rev. Lett. **116**, 166602 (2016).
[13] F. Nichele, M. Kjaergaard, H. J. Suominen, R. Skolasinski, M. Wimmer, B.-M. Nguyen, A. A. Kiselev, W. Yi, M. Sokolich, M. J. Manfra, F. Qu, A. J. A. Beukman, L. P. Kouwenhoven, and C. M. Marcus, arXiv:1605.01241 (2016).
[14] R. Winkler, *Spin-orbit Coupling Effects in Two-Dimensional Electron and Hole Systems* (Springer, Berlin, 2003).
[15] E. McCann and V. I. Fal'ko, Phys. Rev. Lett. **96**, 086805 (2006).
[16] E. V. Castro, N. M. R. Peres, T. Stauber, and N. A. P. Silva, Phys. Rev. Lett. **100**, 186803 (2008).
[17] A. Varlet, D. Bischoff, P. Simonet, K. Watanabe, T. Taniguchi, T. Ihn, K. Ensslin, M. Mucha-Kruczynski, and V. I. Fal'ko, Phys. Rev. Lett. **113**, 116602 (2014).
[18] J. Jung, M. Polini, and A. H. MacDonald, Phys. Rev. B **91**, 155423 (2015).
[19] T. Stauber, N. M. R. Peres, F. Guinea, and A. H. Castro Neto, Phys. Rev. B **75**, 115425 (2007).
[20] S. Wu, X. Dai, H. Yu, H. Fan, and W. Yao, arXiv:1409.4733 (2014).
[21] T. Cao, Z. Li, and S. G. Louie, Phys. Rev. Lett. **114**, 236602 (2015).
[22] E. Berg, M. S. Rudner, and S. A. Kivelson, Phys. Rev. B **85**, 035116 (2012).
[23] J. Ruhman and E. Berg, Phys. Rev. B 90, 235119 (2014).
[24] In other studies[25,26], however, the enhancement of the exchange energy at the singularity point was found to be marginal.
[25] S. Chesi and G. F. Giuliani, Phys. Rev. B **83**, 235309 (2011).
[26] T. Kernreiter, M. Governale, R. Winkler, and U. Zülicke, Phys. Rev. B **88**, 125309 (2013).
[27] See Appendices I to IV for more information.
[28] L. Onsager, Philos. Mag. **43**, 1006 (1952).
[29] Y. Liu, J. Shabani, and M. Shayegan, Phys. Rev. B **84**, 195303 (2011).
[30] Y. W. Suen, J. Jo, M. B. Santos, L. W. Engel, S. W. Hwang, and M. Shayegan, Phys. Rev. B **44**, 5947 (1991).
[31] Y. W. Suen, L. W. Engel, M. B. Santos, M. Shayegan, and D. C. Tsui, Phys. Rev. Lett. **68**, 1379 (1992).
[32] Y. Liu, A. L. Graninger, S. Hasdemir, M. Shayegan, L. N. Pfeiffer, K. W. West, K. W. Baldwin, and R. Winkler, Phys. Rev. Lett. **112**, 046804 (2014).
[33] G. Bastard, *Wave Mechanics Applied to Semiconductor Heterostructures* (Les Editions de Physique, Les Ulis Cedex, 1988).
[34] G. Dresselhaus, Phys. Rev. **100**, 580 (1955).
[35] S. J. Papadakis, E. P. De Poortere, H. C. Manoharan, M. Shayegan, and R. Winkler, Science **283**, 2056 (1999).
[36] Note that, while our samples' nominal QW width is 40 nm, in our calculations we use a width of 38 nm so that the onset of the excited subband occupation, $p = 1.2 \times 10^{11}$ cm^{-2}, matches the experimental value. There are no other adjustable parameters in the calculations.
[37] We show in Appendix III that the magneto-oscillations corresponding to this peak can be extracted via inverse FT.
[38] H. L. Stormer, A. C. Gossard, and W. Wiegmann, Solid State Commun. **41**, 707 (1982).
[39] H. L. Stormer, A. C. Gossard, and W. Wiegmann, J. Vac. Sci. Technol. **21**, 507 (1982).

[40] J. P. Lu, Ph. D. Thesis, Princeton University (1998).
[41] J. P. Lu and M. Shayegan, Phys. Rev. B **58**, 1138 (1998).
[42] M. Shayegan, J. Jo, Y. W. Suen, M. Santos, and V. J. Goldman, Phys. Rev. Lett. **65**, 2916 (1990).
[43] For example, because of the very small area of our annular FS, there could be a "magnetic blurring" of the SdH oscillations[44], or disorder-induced scattering between the inner and outer ring[45].
[44] R. de Gail, M. O. Goerbig, and G. Montambaux, Phys. Rev. B **86**, 045407 (2012).
[45] V. V. Mkhitaryan and M. E. Raikh, Phys. Rev. B **83**, 045406 (2011).
[46] G. Liu, G. Wang, Y.Zhu, H. Zhang, G. Zhang, X. Wang, Y. Zhou, W. Zhang, H. Liu, L. Zhao, J. Meng, X. Dong, C. Chen, Z. Xu, and X. J. Zhou, Rev. Sci. Inst. **79**, 023105 (2008).
[47] J. Shabani, T. Gokmen, Y. T. Chiu, and M. Shayegan, Phys. Rev. Lett. **103**, 256802 (2009).
[48] B. Vinter and A. W. Overhauser, Phys. Rev. Lett. **44**, 47 (1980).
[49] M. E. Raikh and T. V. Shahbazyan, Phys. Rev. B **49**, 5531 (1994).